Published in final edited form as:
*J Pharmacol Exp Ther*. 2008 July ; 326(1): 196–208. doi:10.1124/jpet.108.137455.

# Curcumin Structure-Function, Bioavailability, and Efficacy in Models of Neuroinflammation and Alzheimer's Disease

**Aynun N. Begum**, **Mychica R. Jones**, **Giselle P. Lim**, **Takashi Morihara**, **Peter Kim**, **Dennis D. Heath**, **Cheryl L. Rock**, **Mila A. Pruitt**, **Fusheng Yang**, **Beverly Hudspeth**, **Shuxin Hu**, **Kym F. Faull**, **Bruce Teter**, **Greg M. Cole**, and **Sally A. Frautschy**

*Departments of Medicine (A.N.B., M.R.J., G.P.L., P.K., F.Y., B.H., S.H., B.T., G.M.C., S.A.F.) and Neurology (G.M.C., S.A.F.) and Psychiatry and Biobehavioral Sciences and The Semel Institute (K.F.F.), University of California, Los Angeles, California; Greater Los Angeles Healthcare System, Geriatric Research Education Clinical Center, Sepulveda, California (A.N.B., M.R.J., G.P.L., P.K., F.Y., B.H., S.H., B.T., G.M.C., S.A.F.); Cancer Prevention and Control Program, Moores UCSD Cancer Center, University of California San Diego, La Jolla, California (D.D.H., C.L.R., M.A.P.); and Department of Post-Genomics and Diseases, Division of Psychiatry and Behavioral Proteomics, Osaka University Graduate School of Medicine D3, Osaka, Japan (T.M.)*

## Abstract

Curcumin can reduce inflammation and neurodegeneration, but its chemical instability and metabolism raise concerns, including whether the more stable metabolite tetrahydrocurcumin (TC) may mediate efficacy. We examined the antioxidant, anti-inflammatory, or anti-amyloidogenic effects of dietary curcumin and TC, either administered chronically to aged Tg2576 APP*sw* mice or acutely to lipopolysaccharide (LPS)-injected wild-type mice. Despite dramatically higher drug plasma levels after TC compared with curcumin gavage, resulting brain levels of parent compounds were similar, correlating with reduction in LPS-stimulated inducible nitric-oxide synthase, nitrotyrosine, F2 isoprostanes, and carbonyls. In both the acute (LPS) and chronic inflammation (Tg2576), TC and curcumin similarly reduced interleukin-1β. Despite these similarities, only curcumin was effective in reducing amyloid plaque burden, insoluble β-amyloid peptide (Aβ), and carbonyls. TC had no impact on plaques or insoluble Aβ, but both reduced Tris-buffered saline-soluble Aβ and phospho-c-Jun $NH_2$-terminal kinase (JNK). Curcumin but not TC prevented Aβ aggregation. The TC metabolite was detected in brain and plasma from mice chronically fed the parent compound. These data indicate that the dienone bridge present in curcumin, but not in TC, is necessary to reduce plaque deposition and protein oxidation in an Alzheimer's model. Nevertheless, TC did reduce neuroinflammation and soluble Aβ, effects that may be attributable to limiting JNK-mediated transcription. Because of its favorable safety profile and the involvement of misfolded proteins, oxidative damage, and inflammation in multiple chronic degenerative diseases, these data relating curcumin dosing to the blood and tissue levels required for efficacy should help translation efforts from multiple successful preclinical models.

Neuroinflammation is implicated in the pathogenesis of many neurodegenerative disorders, including Alzheimer's disease (AD). In AD, several mediators in the inflammation cascade contribute both to neurodegeneration and to the production and accumulation of the β-amyloid peptide, including interleukin (IL)-1β, phospho-c-Jun $NH_2$-terminal kinase (pJNK), reactive oxygen species, inducible nitric-oxide synthase (iNOS)-mediated production of reactive nitric oxide species, and lipid peroxidation products (e.g., 8-iso-$PGF_2\alpha$) (for review, see Akiyama

**Address correspondence to:** Dr. Sally A. Frautschy, Departments of Medicine/Neurology UCLA, Greater Los Angeles Healthcare System, VA Medical Center, Research 151, 16111 Plummer St., Sepulveda, CA 91343. E-mail: frautsch@ucla.edu.

et al., 2000). For AD therapeutics, there is rationale to develop drugs that attenuate inflammatory cascades contributing to neurodegeneration and amyloid production or accumulation. However, there is concern that some anti-inflammatory drugs may interfere with phagocytic clearance of amyloid. Curcumin, a compound known to inhibit inflammation while reducing plaque deposition in AD models, is the yellow pigment of the widely used spice, turmeric. Curcumin antagonizes many steps in the inflammatory cascade, including activator protein-1 transcription, activation of nuclear factor-κB, iNOS, and JNK (Pendurthi et al., 1997; Weber et al., 2006). Unlike α-tocopherol (vitamin E), which is a poor scavenger for NO-related oxidation, curcumin exerts potent antioxidant activity for NO-related radical generation (Chan et al., 1998). In contrast to nonsteroidal anti-inflammatory drugs whose adverse side effects include gastrointestinal ulceration and liver or kidney toxicity, curcumin seems to be relatively safe, even in clinical trials for prevention of relapse of ulcerative colitis (Hanai et al., 2006). Curcumin administration has been reported to attenuate cognitive deficits, neuroinflammation, and plaque pathology in AD models (Frautschy et al., 2001; Yang et al., 2005; Garcia-Alloza et al., 2007). Beyond AD, oral curcumin efficacy in vivo has been shown in models for many conditions with oxidative damage and inflammation, including many types of cancer, diabetes, atherosclerosis, arthritis, stroke, peripheral neuropathy, inflammatory bowel, and brain trauma (Aggarwal et al., 2007).

The poor oral absorption of curcumin in both humans and animals has raised several concerns that this may limit its clinical impact (Kelloff et al., 1996). Curcumin is a biphenolic compound with hydroxyl groups at the *ortho*-position on the two aromatic rings that are connected by a β-diketone bridge, containing two double bonds (dienone), which can undergo Michael addition, critical for some of the effects of curcumin (Weber et al., 2006), but contributing to chemical instability in aqueous solution (Pan et al., 1999). Pharmacokinetic studies of curcumin demonstrate extensive intestinal sulfation and glucuronidation (Kelloff et al., 1996; Pan et al., 1999; Ireson et al., 2001; Sharma et al., 2004). Typically, clinical trials show negligible unconjugated curcumin plasma levels with oral dosing (Lao et al., 2006; Baum et al., 2008), leading to the suggestion that in vivo efficacy may come from a more bioavailable and/or potent metabolite (Kelloff et al., 1996).

Potential metabolites, some of which may be active, include tetrahydrocurcumin (TC), hexahydrocurcumin, hexahydrocurcuminol, vanillin, vanillic acid, and ferulic acid (Ireson et al., 2002). However, detectable levels of these metabolites in active unconjugated forms after administration of the parent compound have not been reported, presumably due to their low concentrations, or vulnerability to sulfation, glucuronidation, or hydrolysis (Baum et al., 2008). TC, produced by reduction of dienone double bonds in curcumin, primarily in the intestinal cells (Okada et al., 2001; Ireson et al., 2002), is resistant to hydrolysis (Pan et al., 1999) and a candidate active metabolite. TC has potent antioxidant and anti-inflammatory properties in vitro (Sugiyama et al., 1996; Pan et al., 2000) and in vivo (kidney) (Okada et al., 2001). Because of its activity and putative increased bioavailability, TC has been chronically fed to aging mice, resulting in significantly increased mean and maximum life spans (Kitani et al., 2004). However, since detection methods have not revealed unconjugated TC in plasma (Pan et al., 1999; Okada et al., 2001), the role of TC as a candidate active curcumin metabolite is unclear, and it has not been tested in AD models. Experiments comparing TC and curcumin are also useful to evaluate the functional importance of the dienone bridge of curcumin. In our studies, the purpose was to determine efficacious blood and tissue TC and curcumin levels for in vivo antioxidant, anti-inflammatory, and antiamyloid activity and the importance of the dienone bridge in an acute inflammatory model and a chronic AD model. In the acute paradigm, we investigated the differential impacts of curcumin versus TC on the drug levels in plasma and brain achieved and on the neuroinflammatory responses to an acute inflammatory stimulus (LPS) after different routes of administration. In the chronic model, we investigated curcumin

metabolism and how chronic dietary administration of curcumin or TC modified Aβ and inflammatory parameters in an aging APP*sw* transgenic mouse model of AD.

## Materials and Methods

### Animals and Treatments

Use of animals was approved by the Greater Los Angeles Veterans Administration Institutional Animal Care and Use Committee. In the acute dosing paradigm, C57BL6/J male and female mice (3~4 months of age; $n = 4$) were administered curcumin, TC, or vehicle by gavage (gav), i.p., or i.m., following periodic fasting for two consecutive days as shown in Fig. 1A. One hour after the 2nd day of dosing, mice were administered LPS (0.5 μg/g b.wt.) by i.p. and sacrificed 3 h later. The gav and i.p. doses were each 148 μg (0.4 μmol) of curcumin (Cayman Chemical, Ann Arbor, MI) or TC (Sabinsa Corp., Piscataway, NJ), and the i.m. dose was 74 μg (0.2 μmol). In brief, curcumin for gavage or injection was dissolved in 0.5 N NaOH, diluted to desired concentration, and then it was neutralized in PBS as described previously (Chan et al., 1998). For acute gavage studies, we dissolved curcumin in NaOH to ensure delivery and efficacy at low doses (Chan et al., 1998). However, this method has the disadvantage of exposing curcumin to hydrolysis, which occurs rapidly at neutral pH (Wang et al., 1997). Therefore, to minimize the impact of the major and minor metabolites of curcumin, we neutralized curcumin less than 5 min before gavage. Although it is possible that some effects observed after gavage were in part due to the metabolites such as ferulic acid, 6-(4′-hydroxy-3′-methoxyphenyl)-2,4-dioxo-5-hexenal, or vanillin, it seems unlikely since absorbance levels at 426 nm indicated greater than 90% added curcumin was still present at time of administration, and ferulic acid has poor blood-brain barrier permeability, so it would be unlikely to have a significant impact on brain responses. A similar acute gavage experiment was performed to investigate the impact of fasting on tissue levels of curcumin and TC and responses to LPS ($n = 4$).

Lyophilized TC or curcumin was mixed in chow for the chronic oral dosing paradigm 500 ppm chow (which is equivalent to ~1.25 mg/day or 83 mg/kg b.wt.) using male and female APP*sw* Tg2576 mice (Fig. 1B). Mice were fed these diets ad libitum for 4 months with TC ($n = 5–7$) or curcumin ($n = 5–11$) during the accelerated period of plaque deposition (12–16 months of age). We also fed transgene-negative animals 2000 ppm chow (~10 mg/day or 333 mg/kg b.wt.) to obtain more tissue to study curcumin metabolism. At sacrifice, mice were first anesthetized with pentobarbital (40 mg/kg b.wt. i.p.) for blood sample collection. Blood was drawn from the abdominal aorta into EDTA-containing tubes, and then it was centrifuged at 1600*g* for 20 min at 4°C. Collected plasma was aliquoted and snap-frozen, using liquid nitrogen. Mice were subsequently perfused with PBS, pH 7.4, containing protease inhibitors [20 μg/ml each pepstatin A, aprotinin, phosphoramidon, and leupeptin; 0.5 mM phenylmethylsulfonyl fluoride (PMSF); and 1 mM EGTA]. Brains were removed and dissected, snap-frozen using liquid nitrogen, and then stored at −80°C for further analysis.

### In Vitro Studies

**Aβ Oligomer Treatment of Neurons—**Nonfibrillar high-molecular weight Aβ42 oligomer was prepared as described previously (Yang et al., 2005). In brief, double-lyophilized synthetic Aβ(1–42) peptide was monomerized by solubilization in 1,1,1,3,3,3-hexafluoro-2-propanol (HFIP). Fibril formation was minimized during subsequent HFIP evaporation by adding sterilized water (to achieve stock solution of 315 μg/ml or 63 μM). Fibrils were formed in the solution by continuous stirring (600 rpm) for 48 h at room temperature (25°C). Then, 10 mM $NaHCO_3$ buffer, pH 10 to 11, was added to optimize high-molecular weight Aβ oligomer stability. Oligomers (100 nM) were added to cells for 48 h at 37°C with curcumin (2.5 μM), TC (2.5 μM), curcumin + TC (1.25 μM each), or vehicle. After 48 h, an LDH toxicity assay was performed on culture media using a CytoTox 96 NonRadioactive Cytotoxicity Assay

(Promega, Madison, WI), and absorption was read at 490 nm. Each data point was determined in triplicate.

To evaluate the impact of curcumin and/or TC on Aβ oligomer toxicity, Aβ oligomers were added to SH-SY5Y human neuroblastoma cells plated at 10,000 cells/well in 96-well plates and differentiated in low-serum Dulbecco's modified Eagle's medium (DMEM) with $N_2$ supplement and 10 μM all-*trans*-retinoic acid for 7 days. The medium was removed and replaced with fresh maintenance medium containing 0.1% BSA.

## In Vitro Studies

**LPS Treatment of Microglia and Primary Hippocampal Neurons—**LPS is commonly known to induce iNOS in the CNS in microglia cells, and there is one report that it induces iNOS in neurons, so we investigated the effect of TC and/or curcumin in both primary neurons and a microglial cell line in vitro.

Cultures of cortical neurons from embryonic day 18 Sprague-Dawley rat fetuses were prepared, yielding ~97% neurons and 3% glia. Cells were first grown in B27 medium (containing cytosine arabinoside to minimize glial cell proliferation) supplemented with 25 μM glutamate, 0.5 μM glutamine, 5 U/ml penicillin, 5 mg/ml streptomycin, and 10% fetal bovine serum. Three hours before treatment, neurons were incubated in neurobasal medium, but without B27 and glutamate. Then, cells were preincubated with 2.5 μM curcumin, TC, curcumin + TC, or vehicle for 1 h before adding LPS (1 μg/ml or 100 nM) and harvesting 24 h later. Cells were washed with PBS at 4°C, scraped into 1 ml of PBS, and then centrifuged at 5000 rpm for 5 min. The cell pellet was sonicated in lysis buffer (0.5% SDS, 0.5% deoxycholate, 1% Triton X-100, 150 mM NaCl, and 10 mM $NaH_2PO_4$) with a protease and phosphatase inhibitor cocktail [0.05 mM fenvalerate, 0.05 mM cantharidin, 1 mM sodium vanadate, 1 mM sodium pyrophosphate, 50 mM sodium fluoride, 0.02 mM phosphoramidon, 1 mM EGTA, 0.1 mM EDTA, 0.02 mM leupeptin, 0.0015 mM aprotinin, 0.0145 mM pepstatin A, 0.250 mM PMSF, and 0.5 mM 4-(2-aminoethyl) benzenesulfonyl fluoride hydrochloride]. After incubation at 4°C for 30 min, the samples were again centrifuged (12,000 rpm for 10 min), and the supernatants were collected and used for determining protein concentration (Bio-Rad DC protein assay kit; Bio-Rad, Hercules, CA) and iNOS levels by Western blot.

The BV-2 microglial cell line (a gift from Prof. Jean deVellis, UCLA, Los Angeles, CA), was used to evaluate the impact on iNOS in the brain, since microglia are the primary source of iNOS in the brain. BV-2 cells were cultured in DMEM (Sigma-Aldrich, St. Louis, MO) supplemented with 10% heat-inactivated fetal bovine serum (Invitrogen, Carlsbad, CA) at 37° C in 5% $CO_2$ in a humidified cell incubator. One day before treatment, serum was removed, and cells incubated in 0.1% BSA and DMEM. Then, cells were pretreated with curcumin, TC, curcumin + TC, or vehicle 1 h before LPS, and cells harvested 24 h later, as described above for cortical neuron cultures.

**MC65 Neuroblastoma Cells—**We also investigated the neuro-protective effects of TC or curcumin on inducible intraneuronal expression of APP C99. MC65 cells were kindly provided by L. W. Jin (University Washington, Seattle, WA). In brief, for cell viability experiments, cells were plated onto 96-well plates at 25,000 cells/well in DMEM (Invitrogen) plus 10% fetal calf serum and 1 μg/ml tetracycline. Twenty-four hours later, cell medium was replaced with tetracycline free Opti-MEM (Invitrogen). Then, cells were treated for 3 days with and without 2 μM curcumin and TC in 0.1% ethanol. After 72 h, 3-(4,5-dimethylthiazol-2-yl)-2,5-diphenyltetrazolium reduction viability assay was performed at 550 nm.

**Plasma and Tissue Sample Preparation for HPLC—**Mouse plasma and brain samples were extracted in 95% ethyl acetate/5% methanol and analyzed by HPLC with detection at 262

(curcumin) and 282 (TC) nm, using 17β-estradiol as an internal standard as described previously but with the following modifications (Heath et al., 2003, 2005). For brain tissue sample preparation, whole brains were first homogenized in 10 volumes of 1 M ammonium acetate, pH 4.6. The extraction efficiency for curcumin and TC was 88 to 97% and 82 to 90% from plasma and brain homogenate, respectively. Using the HPLC method, the lower limits of detection for Curc were 35 ng/ml (95.1 nM) in plasma and 100 ng/g wet tissue (271 nM) in brain, and for TC they were 8 ng/ml (21.5 nM) in plasma and 250 ng/g wet tissue (672 nM) in brain.

**Curc and TC LC/MS/MS Analysis of Brain from Chronically Fed Mice—**Methods for assessing efficacy of drugs for antioxidant, anti-inflammatory, and anti-amyloid activity used considerable brain tissue, so there was limited tissue available to assess brain concentrations of parent drug and metabolites. Therefore, we developed a more sensitive, efficient, and specific method to evaluate curcumin metabolism and levels in the brain after chronic feeding.

The curcumin-related compounds monitored by LC/tandem mass spectrometry (MS/MS) were curcumin, tetrahydrocurcumin, and tetramethoxycurcumin (the internal standard). All gave strong signals for the $[M–H]^-$ ion in negative ion electrospray mass spectrometry when infused in solutions of water/acetonitrile containing 10 mM ammonium acetate. The MS/MS of these ions produced a number of fragment ions, the most intense of which were selected for quantitation by MS/MS-multiple reaction monitoring (MRM).

Dried extracts were redissolved in acetonitrile/methanol/water/acetic acid (41:23:36:1, all by volume), and an aliquot of the solution (typically 100 μl) was injected onto a reverse phase HPLC column (Ascentis Express C18, 150 × 2.1 mm; Supelco, Bellefonte, PA) equilibrated in 10 mM ammonium acetate (buffer A) and eluted (100 μl/min) with an increasing concentration of acetonitrile/isopropanol [1:1 (v/v) buffer B: min/% B; 0:10, 5:10, 30:100, and 33:100]. The effluent from the column was passed directly to an Ionspray ion source connected to a triple quadrupole mass spectrometer (API $III^+$; PerkinElmerSciex Instruments, Boston, MA) operating in the negative ion MS/MS MRM mode in which the intensity of parent-to-fragment ion transitions was recorded with an orifice voltage of 65 and argon collision gas (instrumental setting collisionally activated dissociation gas thickness of 120). The *m/z* values of the specific transitions were for curcumin, 367.1→271.1, 367.1→173.1, 367.1→149.0; for tetrahydrocurcumin, 371.1→235.1; and for tetramethoxycurcumin, 395.2→380.2, 395.2→365.1, (the internal standard). To enhance signal intensity for low-abundance samples, both Q1 and Q3 were detuned so that the isotope clusters for the polypropylene calibrant ions between *m/z* 200 and 1000 were not separated from one another. This strategy resulted in a signal enhancement for the curcumin-related compounds between 3.4- and 8-fold. Instrument manufacturer-supplied software was used to calculate peak heights (MacSpec version 3.3; PerkinElmerSciex Instruments). For quantitation, the most intense of the parent→fragment transitions for each compound were used. These were 367.1→149.0 for curcumin and 395.2→365.1 for tetramethoxycurcumin (the internal standard).

MRM sensitivity was routinely checked with injections of 0.01, 0.1, and 1 pmol of each of the curcuminoid compounds. At maximal sensitivity (detuned mass spectrometric conditions), the limit of detection corresponded to 100 pg/g wet tissue of extracted material or 272 pM for curcumin and 1 ng/g wet tissue or 2.68 nM for tetrahydrocurcumin. Injection of 0.1 pmol for each compound gave strong signals, with peak height/baseline noise ratios in excess of 50:1. The retention time of Curc, TC, and internal standard was 28.24, 26.36, and 30.27 min, respectively.

**Quantitative PCR—**Brain levels of iNOS mRNA were measured by reverse transcription followed by quantitative PCR. In brief, total RNA was isolated from brain using the RNAqueous kit (Ambion, Austin, TX) as per the manufacturer's instructions, and it was treated with DNase. RNA (1 μg) was then reverse-transcribed with dT primers, using the Retroscript kit, and it was aliquoted for single uses. The analysis of mRNA levels was performed using QPCR with the SYBR Green PCR Master Mix (Applied Biosystems, Foster City, CA) in an SDS7700 thermocycler (Applied Biosystems), followed by a dissociation curve analysis that verified the amplification of a single PCR species. Thermocycling parameters were standard for the SDS7700 (Applied Biosystems) instruments: 95°C for 10 min, and 40 cycles of 95°C for 15 s and 60°C for 1 min. Each sample was tested in triplicate. A standard curve was run to allow relative comparisons of the sample values. The PCR primers for iNOS were 5′-TGAGACAGGAAAGTCGGAAG-3′ (forward) and 5′-TCCCATGTTGCGTTGGAA-3′ (reverse), and they were normalized to glyceraldehyde-3-phosphate dehydrogenase mRNA levels (an internal housekeeping gene control) for each cDNA sample, using the primers from the TaqMan Rodent glyceraldehyde-3-phosphate dehydrogenase control reagents (Applied Biosystems).

**Tissue Extraction and ELISAs for Aβ, 8-Iso-PGF$_{2}$α (F2 Isoprostanes), and IL-1β—**For Aβ and IL-1β ELISAs, an aliquot of frozen brain tissue (powderized on dry ice with a mortar and pestle) was homogenized in 10 volumes of TBS containing the protease inhibitor cocktail (first without detergents). Samples were sonicated briefly and centrifuged at 100,000*g* for 20 min at 4°C. The TBS-extracted supernatant was analyzed by ELISA for interleukin 1β and Aβ to measure an inflammatory endpoint and levels of "soluble Aβ," respectively. To evaluate "insoluble Aβ," the pellet was dissolved in guanidine and analyzed by Aβ ELISA as described previously (Lim et al., 2000). For F2 isoprostane ELISA, a separate aliquot of powderized tissue was used, and total lipids were extracted as described previously and measured using, the 8EPI-F2 Immunoassay kit (Oxford Biomedical Research, Oxford, MI) (Frautschy et al., 2001).

**Western Blot for Brain iNOS, pJNK, Nitrotyrosine, and Carbonyls—**To detect iNOS, nitrotyrosine, and pJNK, the TBS fraction was used. Samples (20 μg) were electrophoresed onto a 10% Tris-glycine gel. After transfer of proteins to polyvinylidene difluoride membrane, blot was blocked for 1 h at room temperature in 5% milk with 0.05% Tween 20 in PBS. The membrane was incubated with primary mouse monoclonal antibodies at 1:1000 dilution overnight at 4°C: anti-iNOS antibody (BD Biosciences Transduction Laboratories, Bedford, MA), anti-nitrotyrosine (Cayman Chemical), or anti-pJNK (Cell Signaling Technology Inc., Beverly, MA). The secondary antibody was horseradish peroxidase-conjugated anti-mouse (1:30,000) incubated for 1 h at room temperature and developed with enhanced chemiluminescence.

For measurement of carbonyls, we used the "Oxyblot" kit (Serologicals Corp., Norcross, GA) as described previously (Lim et al., 2001). The TBS-insoluble pellet was sonicated in lysis buffer (see above) with protease inhibitor cocktails, and then it was centrifuged at 100,000*g* for 20 min at 4°C. The resultant supernatant was collected as the "lysis fraction." Next, 10 μg of protein from this fraction was reacted with 1X dinitrophenylhydrazine for ~15 to 30 min, followed by neutralization with a solution containing glycerol and β-mercaptoethanol. These samples were electrophoresed on a 10% Tris-glycine gel, transferred, and blocked. The blot was incubated overnight with a rabbit anti-dinitrophenylhydrazine antibody (1:150) at 4°C, followed by incubation in goat anti-rabbit (1:300) for 1 h at room temperature. Bands were visualized using chemiluminescent techniques with non-saturating exposures, and the resulting bands were scanned and quantified using a densitometer and Molecular Analyst software (model GS-700; Bio-Rad).

**Immunostaining and Image Analysis—**In addition to analyzing Aβ and GFAP by Western of dissected brain homogenates, brains were also analyzed immunohistochemically. Hemibrain cryosections (8 μm in thickness) of Tg2576 mice on curcumin or TC diet were analyzed immunohistochemically from the anterior middle and posterior hippocampal bregma regions for Aβ (rabbit polyclonal antibody; 1:500 anti-Aβ1-13, DAE) or GFAP (1:10,000, monoclonal antibody; Sigma-Aldrich) as described previously (Lim et al., 2000). In brief, antigen retrieval was accomplished by steaming sections in an unmasking solution (Vector Laboratories, Burlingame, CA). After quenching with 0.6% hydrogen peroxide and blocking with normal serum, sections were incubated with primary antibodies overnight at 4°C. After incubating with the peroxidase-containing ATP-binding cassette reagent (Vector Laboratories), sections were developed with metal-enhanced diaminobenzidine (Pierce Chemical, Rockford, IL).

Acquired images of anti-Aβ (DAE) or GFAP-stained sections were analyzed using NIH Image public domain software (National Institutes of Health, Bethesda, MD) to calculate number of plaques, plaque burden, and percentage of GFAP-area stained in cortical and hippocampal layers. Statistical analysis of variables was by 2 × 2 ANOVA (treatment × region).

**Aβ42 Aggregation Assays by Western Blot and Oligomer Disaggregation by A11 Dot Blot Assay—**We investigated the impact of TC and curcumin on aggregation using two different preparations of oligomer starting with lyophilized Aβ42, monomerized with HFIP. The first oligomer was prepared by incubating 5 μM Aβ for 4 h at 37°C in F12 media, and the second oligomer was prepared by incubating 67 μM Aβ in water at 48 h at room temperature and then running the preparations that had been coincubated with different concentrations of TC or curcumin on a Western immunoblotted with 6E10 anti-Aβ antibody as described previously (Yang et al., 2005). We also examined the impact of TC and curcumin on Aβ42 disaggregation in a cell-free system, using a dot blot with an oligomer-specific antibody as described previously (Yang et al., 2005) except oligomers were preformed. Freshly prepared Aβ42 oligomers (11 μM; provide by Dr. Charles C. Glabe, University of California, Irvine, CA) were coincubated with curcumin (16 μM), TC (16 μM), curcumin + TC (curcumin and TC together, 8 μM each), or vehicle for 72 h at 25°C, and then 500 ng per well was applied to the nitrocellulose membrane in a Bio-Dot apparatus (Bio-Rad). The membrane was blocked with 10% nonfat milk in TBS-T at room temperature for 1 h, washed with TBS-T, and probed with either the anti-Aβ (6E10) or the anti-oligomer A11 antibody (Yang et al., 2005) (1:10,000) in 3% BSA-TBS-T overnight at 4°C. After washing, it was probed with anti-rabbit horseradish peroxidase-conjugated antibody (Pierce Chemical) solution (1:12,000) for 1 h at room temperature. The blot was developed with SuperSignal (Pierce Chemical) for 2 to 5 min. Dots were scanned and analyzed with a model GS-700 densitometer using Molecular Analyst software (Bio-Rad).

**Statistical Analysis—**The comparative effects of curcumin and TC treatment were analyzed by one-way ANOVA analysis, followed by post hoc Bonferroni/Dunn test. All Western blot densitometry was analyzed by one-way ANOVA analysis (InStat version 3.05; Graph-Pad Software Inc., San Diego, CA) and image analysis by 2 × 2 ANOVA (treatment × region) at anterior, middle, and posterior hippocampus, four consecutive sections per bregma. Coefficient of correlation and significance of the degree of linear relationship between parameters were determined with a simple regression model using StatView (Abacus, Berkeley, CA; discontinued) or JMP (SAS Institute, Cary, NC) software. All experiments were performed in triplicate or quadruplicate. GraphPad Prism software version 5.00 (GraphPad Software Inc.) was used to evaluate the dose-response curves, and $EC_{50}$ values for responses in iNOS, IL-1β, and isoprostane. The drug-response curves were determined by using nonlinear regression. For Fig. 3 and Fig. 4, the concentration of drug is shown in log 10 scale in *x*-axis and curve fit determined using a variable slope model. The response variable was normalized,

according to the percent maximal response. The curves for the effect of Curc or TC on iNOS, IL-1β and isoprostane were fitted using the equation $Y = 100/(1 + 10\text{^}((\log EC_{50} - X) \times \text{Hill slope}))$.

## Results

Previous measurements of curcumin or TC using our published HPLC methods showed detection of TC or curcumin in tissue samples spiked with TC or curcumin. However, it was not known whether these methods were sufficiently sensitive or specific to detect unconjugated TC or curcumin in animals treated with curcumin or TC before sacrifice. We delivered curcumin or TC using three routes of administration to investigate the impact of GI tract on tissue levels and drug efficacy. The structures of curcumin and TC are shown in Fig. 2, A and B, respectively, illustrating that the double bonds if curcumin flanking the β-diketone bridge are lost upon reduction to TC. Data demonstrated successful detection of these compounds in treated mice (Fig. 2; Table 1). Representative chromatograms from brains or plasma of vehicle-treated mice showed the internal standard peak, without signal for curcumin or TC, respectively (Fig. 2, C and D). However, when mice were injected i.m. with either drug, their respective peaks were present in both brain (Fig. 2, E and F) and plasma fractions (Fig. 2, G and H).

We also examined metabolism of curcumin. Although in the acute study we did not detect metabolites of curcumin in the brain or plasma, measurable levels were obtained in the chronic study. HPLC analysis revealed that plasma containing the parent compound curcumin (Fig. 2I) also contained the metabolite TC (Fig. 2J; Table 2). The plasma values for the metabolite of mice fed 500 ppm curcumin were close to the lower limit of detection, but they were higher in animals fed a higher dose (2000 ppm). Likewise, the metabolite was also detected by LC/MS/MS in the brains of mice chronically fed the parent compound curcumin, using LC/MS/MS (Fig. 2K; Table 2). Brain levels of the metabolite were approximately 6-fold less than that of the parent compound (Table 2).

Table 1 (acute study) shows that plasma levels of drug are higher with TC than with curcumin, regardless of route of administration. Similar results are observed in chronic study (Table 2).

Brain-to-plasma ratios of parent compounds were calculated. In the acute gavage study (Table 1), curcumin ratios were approximately 5-fold higher in brain than plasma), whereas TC brain-to-plasma ratios were much lower (Table 1), particularly in chronically fed mice (where brain TC levels were ~0.5-fold that of plasma; Table 2).

Brain levels of the curcuminoids ranged from 0.7 to 6 μM for TC and from 1.4 to 3 μM for curcumin, depending on route of administration. We then assessed the association of these brain levels with anti-inflammatory effects, using iNOS as an index of inflammation. We induced inflammation by injecting LPS (i.p.), and then we analyzed brains of TC- or curcumin-treated mice for iNOS protein (Fig. 3, A and B) and mRNA (Fig. 3C). LPS caused robust increases in iNOS protein and mRNA. Although i.m. injection, which produced the highest brain drug levels, tended to be slightly more effective in attenuating these LPS responses, all routes of administering curcumin and TC caused large decreases in iNOS protein and mRNA. Regression analysis showed a close correlation between inhibition of iNOS mRNA and increasing concentrations of the administered curcuminoids (Fig. 3D). The $EC_{50}$ value for iNOS mRNA inhibition in vivo was 1.186 and 0.701 μM for curcumin and TC, respectively.

Because LPS induces CNS expression of IL-1β (Hsu and Wen, 2002), an inflammatory cytokine known to be elevated in neuroinflammatory diseases, including AD (Akiyama et al., 2000), we evaluated the relative impact of curcumin or TC on IL-1 β induction. Although LPS effectively induced robust elevations in IL-1 β brain levels compared with vehicle, all routes of administration of either curcumin or TC equally inhibited this response (Fig. 4A). The

$EC_{50}$ value for IL-1β inhibition in vivo was 1.722 and 1.286 μM for curcumin and TC, respectively (Fig. 4B).

LPS can induce brain lipid peroxidation, as measured by oxidation of arachidonic acid to F2 isoprostanes, which are elevated in AD and correlate with synaptic loss and (Montine et al., 2004) and AD models (Frautschy et al., 2001). Therefore, we investigated the impact of curcumin or TC on induction of F2 isoprostanes. Results showed that LPS increased F2 isoprostanes. Although acute oral delivery of curcumin or TC failed to produce brain levels sufficient to modify isoprostanes, i.p. delivery slightly reduced, and i.m. delivery greatly reduced LPS-induced F2 isoprostanes (Fig. 4C). The $EC_{50}$ value for F2 isoprostane inhibition in vivo was 1.067 and 0.501 μM for curcumin and TC, respectively (Fig. 4D).

Superoxide reaction with nitric oxide, resulting in increased peroxynitrite, typically occurs in neuroinflammatory diseases such as AD (Castegna et al., 2003). An indirect index of peroxynitrite can be estimated by measuring anti-nitrotyrosine (NT)-reactive proteins, formed by peroxynitrite-mediated nitration of protein tyrosine residues. Results demonstrated that LPS induced prominent 75- and 90-kDa NT-reactive bands, but gavage with either compound was not effective in modifying NT (Fig. 5A), similar to the failure of gavage to suppress F2 isoprostane induction. In contrast, curcumin was effective in suppressing LPS-induced protein oxidation, as measured by carbonyls, regardless of route of administration (Fig. 5B), unlike TC that was only effective in reducing carbonyl induction if injected by i.m. (Fig. 5C).

Because it has been reported that fasting may enhance absorption or use of curcumin (Chan et al., 1998), and because chronic treatment is likely necessary for therapeutic intervention of diseases, we evaluated the impact of food ad libitum on curcumin and TC plasma and brain levels. We increased the gavage dose to 480 μg, which is closer to the daily dietary consumption of curcumin used to reduce AD pathogenesis in the Tg2576 mouse (Lim et al., 2001). Compared with fasted mice, mice previously fed ad libitum showed a large reduction in absorption of both curcumin and TC (by gavage) as measured by their contents in the brain (Fig. 6A). TC was not detectable in brain if given with food, and curcumin was detectable, but reduced. The diminished plasma levels associated with food intake correlated with impaired (curcumin) or abolished (TC) efficacy in inhibition of LPS-induced brain iNOS (Fig. 6B).

Because curcumin was not detectable with acute gavage dosing with food (nonfasted), we then investigated whether it could be detected after chronic administration in chow. We chose doses previously shown to reduce oxidative damage, neuroinflammation and plaque pathology in the APP*sw* Tg2576 mouse (Lim et al., 2001). Table 2 shows that in contrast to acute gavage, chronic oral dosing in diet of curcumin or TC resulted in detectable plasma levels of 0.095 and 0.73 μM, respectively. Like acute dosing, chronic dosing resulted in plasma levels of TC that were severalfold higher than those of curcumin.

We then evaluated the relative efficacies of curcumin- and TC-fed mice on plaque pathology in the Tg2576 APP*sw* mouse during plaque deposition (12–16 months of age). Immunostaining for anti-Aβ revealed that, compared with control-fed mice, curcumin-fed mice showed a marked reduction in plaques (Fig. 7, A–D), similar to that described previously (Lim et al., 2001). But this was not observed with TC-fed mice (Fig. 7, E and F). Quantitation of plaque size (Fig. 7G) and plaque burden (Fig. 7H) confirmed that curcumin, but not TC, reduced Aβ pathology. We then analyzed the dissected cortex for Aβ levels, and we showed that curcumin-fed, but not TC-fed animals had reduced Aβ in the insoluble fraction (Fig. 7I). The only significant impact of TC on Aβ variables was on soluble Aβ, which it reduced more than curcumin (Fig. 7J).

GFAP was analyzed immunohistochemically to evaluate the impact of curcumin and TC on the elevated gliosis in this transgenic model of AD (Fig. 8, A–H). Quantitation of GFAP

confirmed the known induction of GFAP in this transgenic model. Both curcumin and TC significantly attenuated the gliosis associated with the transgene (Fig. 8I). IL-1β is an index of neuroinflammation, thought to contribute to AD pathogenesis, and it was elevated in this model. Like gliosis, IL-1β was effectively reduced by both curcumin and TC compared with Tg+ mice on the control diet (Fig. 9A). However, although carbonyls known to be induced by this transgene (Lim et al., 2001) were reduced by curcumin as described previously, TC showed only a nonsignificant trend for reducing carbonyls (Fig. 9B). Given that the stress-activated pJNK has been reported to be elevated in cortical homogenates of this model (Puig et al., 2004) and JNK is a putative target of curcumin, we also examined the relative impacts of curcumin and TC on pJNK. Western analysis showed two bands at 46 and 56 kDa, which when quantified demonstrated that both curcumin and TC effectively reduced pJNK, with TC being particularly potent (Fig. 9, C and D). Because of data suggesting that pJNK may influence Aβ, we evaluated the association by a regression analysis, and we showed that the degree of TBS soluble Aβ reduction was proportional to that of pJNK reduction (Fig. 9E).

In vitro data confirmed that both TC and curcumin were potent suppressors of iNOS in primary neurons (Fig. 10A) and in BV2 microglia (data not shown). Both protected from oligomeric Aβ toxicity in a neuroblastoma model as measured by LDH (Fig. 10B). In contrast, using a model of intraneuronal APP C99 fragment accumulation (M-65 cells, provided by L. W. Jin; APP mutation lacking leader sequence), only TC protected from intraneuronal Aβ toxicity, possibly indicating differing neuroprotective mechanisms of TC and curcumin (Fig. 10C). We then investigated the impact of TC and curcumin on Aβ oligomer formation (Fig. 10, D–F). Aggregating Aβ at low concentrations was robustly attenuated by curcumin, but not by TC (Fig. 10D), similar to previous data (Yang et al., 2005). Although TC had no impact on aggregation of Aβ at the lower concentration, at the higher Aβ concentration, TC seemed to selectively reduce aggregates of the intermediate molecular mass oligomers (30–200 kDa; Fig. 10E) and also the level of preaggregated oligomers (11 μM) in a cell-free dot blot assay using oligomer-specific A11 (Fig. 10F). Unlike curcumin, TC seemed to increase (rather than reduce) very high aggregates associated with the stack (Fig. 10E). When curcumin (but not TC) was added to preaggregated oligomers, intense monomeric bands occurred, suggesting deaggregation (data not shown).

## Discussion

We demonstrate target plasma and brain levels needed for in vivo antioxidant, anti-inflammatory, and anti-Aβ activities of TC and curcumin, which is relevant to clinical utility and the functional aspects of the molecular structure. Evidence supports similar mechanisms of TC versus curcumin on neuroinflammatory cascades but a differential mechanism on amyloid pathogenesis.

### Curcumin Metabolism to TC

We demonstrate for the first time that mice chronically fed the parent compound curcumin showed detectable levels of the unconjugated metabolite TC in both the plasma and brain. Curcumin is reduced to TC by the intestinal cells as the major metabolite (Ireson et al., 2002), but only the unglucuronidated metabolite was detected in mice (Pan et al., 1999; Okada et al., 2001; Liu et al., 2006) or humans (Baum et al., 2008) administered curcumin. One explanation for the discrepancy might be our improved sensitivity of the HPLC (Heath et al., 2005) and LC/MS/MS assays. Brain concentrations of the parent compound were approximately 6 to 10-fold higher than levels of the metabolite, depending on curcumin dose.

### Differential Brain Plasma Ratios for TC versus Curc

Plasma TC levels were nearly 8-fold higher than curcumin levels after chronic dosing (with food), consistent with either TC having better GI absorption or greater stability than curcumin (Okada et al., 2001). However, fasting increased plasma curcumin levels, consistent with a previous report (Chan et al., 1998). Fasting also increased TC plasma levels. Fasting slows stomach emptying and gastric motility, so it could result in an increase in absorption from the stomach, as opposed to the small intestine where glucuronidation is thought to occur. However, the relatively high plasma TC levels cannot be attributed solely to improved GI absorption, since injections of TC also resulted in comparatively high plasma levels. Thus, these observations are more likely due to the resistance of TC to hydrolysis in plasma, consistent with in vitro stability data and similarly high glucuronidation rates (Pan et al., 1999; Okada et al., 2001).

Brain-to-plasma ratios from acute studies were highest for curcumin, suggesting its stability in lipid-rich compartments, where hydrolysis is limited. In the chronic study with 500 ppm, the brain-to-plasma ratio dropped for TC and increased for curcumin. This may reflect differences in blood-brain barrier transport, or brain or plasma clearance. For example TC may be more readily exported from brain or less stable in the brain than curcumin. Although curcuminoid entry into the brain is limited by glucuronidation, both TC and curcumin are readily glucuronidated. Thus, glucuronidation cannot explain the different brain-to-plasma ratios.

### Effects of TC and Curcumin on Brain Inflammation

Curcumin and TC similarly inhibited IL-1β in the acute inflammation model (1.722 and 1.286 μM) and IL-1β and the astrocytic marker GFAP in the chronic AD model (at 1.3 and 0.7 μM, respectively). It was reported previously that curcumin reduced CNS IL-1β (Lim et al., 2001; Chainani-Wu, 2003), but this is the first demonstration that TC reduced brain IL-1β. Likewise, both compounds strongly inhibited LPS induction of iNOS protein and mRNA. The anti-inflammatory activity of curcumin is mediated by limiting the activity of transcription factors (Weber et al., 2006), or coactivators of activator protein-1, including p300 histone acetyltransferase (Marcu et al., 2006)). Our data support the hypothesis that the phenolic ring methoxy groups, but not the C=C double bonds of the dienone of curcumin, mediate anti-inflammatory effects in vivo.

### Antioxidant Effects of TC and Curcumin

Curcumin inhibited protein oxidation better than TC in the AD model. Previously, the brain antioxidant effects of curcumin have been well documented in models of cerebral ischemia (Thiyagarajan and Sharma, 2004), AD (Lim et al., 2001), and brain trauma (Wu et al., 2006). Although the 4-hydroxyl-3-methoxy phenolic groups, which are common to both TC and curcumin are critical for some antioxidant effects, metal chelation can also reduce oxidative damage (Cherny et al., 2001), which along with amyloid reduction might contribute to the slightly better antioxidant effects of curcumin in the Tg2576 model. The present report is the first showing TC efficacy on CNS oxidative damage.

### TC and Curcumin Effects on Aβ and JNK in the Tg2576 Mouse

Curcumin was more effective than TC in attenuating plaque pathogenesis, demonstrating an important difference between the two compounds. The inhibitory effect of curcumin on fibril and oligomer formation and disaggregation was consistent with previous reports (Kim et al., 2005; Yang et al., 2005). It is also consistent with in vitro data showing that, although addition or removal of the phenolic ring methoxy groups did not attenuate potency of curcuminoids in reducing fibril formation, loss of the dienone double bonds resulted in loss of fibril inhibition

(Kim et al., 2005). Curcumin readily metabolizes to ferulic acid, which also affects fibril formation; however, the $EC_{50}$ concentrations for disaggregation of fibrillar Aβ is approximately 10-fold higher for ferulic than for curcumin (Ono et al., 2005), arguing against a substantial role for this charged and likely poorly brain-permeant metabolite. Factors such as metal chelation, which is known to reduce plaque formation, may contribute to the more potent plaque-reducing effects of curcumin in vivo (Cherny et al., 2001). Curcumin, but not TC, readily binds $Cu^{2+}$ and $Fe^{2+}$, and it may remove metal from Aβ (Baum et al., 2008).

Our data showing curcumin reduction in soluble Aβ levels confirmed our previous report showing a similar 50% reduction (Lim et al., 2001). Our soluble (TBS) Aβ levels in aged Tg2576 were well above baseline Aβ monomer production levels in Tg2576, and they clearly included soluble aggregates (oligomers) as shown on Westerns. It might be presumed that, if insoluble and soluble Aβ compartments were in equilibrium, drugs reducing Aβ aggregation or increasing Aβ clearance would similarly reduce both amyloid fibrillar plaques and soluble oligomers, as we observed for curcumin. However, this was not the case with TC. The surprising finding was that despite TC having no statistically significant impact on plaque burden, it reduced soluble Aβ by 75% (Fig. 7J). One possibility is that, despite the greater affinity of curcumin for fibrils (Kim et al., 2005), TC and curcumin have similar affinity for oligomers as suggested by our cell-free aggregation studies. Another possibility is that the TC reduction of soluble Aβ related to the observed stronger inhibition of pJNK. Aβ levels can be lowered by pJNK inhibitors (Borsello and Forloni, 2007) or in JNK knockout mice crossed with APP Tg mice in vivo (Prof. Reinhard Schleibs, University of Leipzig, Germany, unpublished observations). Soluble Aβ seems to more closely correlate with synaptic loss and neurodegeneration in AD (Frautschy et al., 2001). Curcumin does not interact directly with JNK, but via unknown mediators upstream to stress-activated kinase 1, mitogen-activated protein kinase kinase kinase 1, or hematopoietic progenitor kinase 1 (Chen and Tan, 1998). JNK is a τ kinase hypothesized to mediate end-stage neurodegeneration and LTP deficits in AD models (Puig et al., 2004; Wang et al., 2004). In summary, although TC was not as effective in reducing brain oxidation and plaque burden, its slightly better impact on reducing soluble Aβ and pJNK merits its further consideration potential clinical use.

In conclusion, curcumin, but not TC reduced plaque burden and protein oxidation in the AD model, demonstrating the importance of the hydrolysis-vulnerable dienone bridge in the anti-amyloid action of curcumin. In contrast, both drugs had similar potent effects on neuroinflammation and CNS pJNK, showing that the phenolic rings, but not the dienone bridge are required for suppression of these targets, which is not simply secondary to amyloid reduction. Overall, our data support the concept of pleiotropic anti-amyloid, antioxidant, and anti-inflammatory treatment for AD. Efficacious tissue levels can be achieved with chronic oral 500 ppm curcumin, which is well within the safety range established in chronic animal experiments by the National Toxicology Program (Kelloff et al., 1996). Similar levels are likely needed to control inflammation, oxidative damage, and protein aggregation in other diseases. However, in humans high oral dosing fails to achieve detectable plasma levels (Lao et al., 2006). The reported failure to achieve these modest target levels in humans with oral supplements predicts limited success in translating to the clinic. In our studies, increasing curcumin solubility with phosphatidyl choline, olive oil, or stearic acid increases plasma and brain levels compared with administering unformulated curcumin powder. For example, oral gavage of an optimized, lipidated curcumin formulation (Verdure Sciences, Noblesville, IN; www.verduresciences.com) resulted in 11-fold higher levels of curcumin in plasma and 4-fold higher levels in brain compared with equal doses of curcumin powder or curcumin-piperine extracts. A 5-mg curcumin dose delivered by acute gavage in this lipid rich formulation ($n$ = 5) resulted in 2.15 ± 0.744 μM mouse brain curcumin levels after 3 h. After 2 weeks of lipidated formulation at 500 ppm curcumin in chow ($n$ = 5), we observed 5.79 ± 1.22 μM mouse brain curcumin, well above the 1 to 2 μM range of $EC_{50}$ concentrations for the inhibition of iNOS,

IL-1β, $PGE_2$, and isoprostanes. This suggests oral delivery can achieve our target tissue levels. Finally, the traditional method of dissolving turmeric in fat during cooking is likely an effective method to improve absorption, and it could play a role in India's low incidence and prevalence of Alzheimer's disease (Lim et al., 2001 and references therein).

## Acknowledgments

We thank Walter Beech for preparation of primary neuron cultures, M65 neuroblastoma, and BV-2 cells. We are grateful to Drs. C. Glabe and Rakez Kayed (University of California, Irvine) for oligomeric-specific polyclonal antibody, to Prof. Jean deVellis for BV-2 cells, and to Prof. Lee Way Jin for M65 cells.

This study was supported by Grant U01028583 (to S.A.F.), VA Merit Grants AG021975 (to S.A.F.) and AG016570 (Cummings Project 1; to G.M.C.). We are grateful for the original support of K. K. Siegel on curcumin in 1998 on a UCLA Pilot Center on Aging Grant.

## References

Aggarwal BB, Sundaram C, Malani N, Ichikawa H. Curcumin: the Indian solid gold. Adv Exp Med Biol 2007;595:1–75. [PubMed: 17569205]

Akiyama H, Barger S, Barnum S, Bradt B, Bauer J, Cole GM, Cooper NE, Eikelenboom P, Emmerling M, Fiebich BL, et al. Inflammation and Alzheimer's disease. Neurobiol Aging 2000;21:383–421. [PubMed: 10858586]

Baum L, Lam CW, Cheung SK, Kwok T, Lui V, Tsoh J, Lam L, Leung V, Hui E, Ng C, et al. Six-month randomized, placebo-controlled, double-blind, pilot clinical trial of curcumin in patients with Alzheimer disease. J Clin Psychopharmacol 2008;28:110–113. [PubMed: 18204357]

Borsello T, Forloni G. JNK signalling: a possible target to prevent neuro-degeneration. Curr Pharm Des 2007;13:1875–1886. [PubMed: 17584114]

Castegna A, Thongboonkerd V, Klein JB, Lynn B, Markesbery WR, Butterfield DA. Proteomic identification of nitrated proteins in Alzheimer's disease brain. J Neurochem 2003;85:1394–1401. [PubMed: 12787059]

Chainani-Wu N. Safety and anti-inflammatory activity of curcumin: a component of tumeric (*Curcuma longa*). J Altern Complement Med 2003;9:161–168. [PubMed: 12676044]

Chan MM, Huang HI, Fenton MR, Fong D. In vivo inhibition of nitric oxide synthase gene expression by curcumin, a cancer preventive natural product with anti-inflammatory properties. Biochem Pharmacol 1998;55:1955–1962. [PubMed: 9714315]

Chen YR, Tan TH. Inhibition of the c-Jun N-terminal kinase (JNK) signaling pathway by curcumin. Oncogene 1998;17:173–178. [PubMed: 9674701]

Cherny RA, Atwood CS, Xilinas ME, Gray DN, Jones WD, McLean CA, Barnham KJ, Volitakis I, Fraser FW, Kim Y, et al. Treatment with a copper-zinc chelator markedly and rapidly inhibits beta-amyloid accumulation in Alzheimer's disease transgenic mice. Neuron 2001;30:665–676. [PubMed: 11430801]

Frautschy SA, Hu W, Miller SA, Kim P, Harris-White ME, Cole GM. Phenolic anti-inflammatory antioxidant reversal of Aβ-induced cognitive deficits and neuropathology. Neurobiol Aging 2001;22:993–1005. [PubMed: 11755008]

Garcia-Alloza M, Borrelli LA, Rozkalne A, Hyman BT, Bacskai BJ. Curcumin labels amyloid pathology in vivo, disrupts existing plaques, and partially restores distorted neurites in an Alzheimer mouse model. J Neurochem 2007;102:1095–1104. [PubMed: 17472706]

Hanai H, Iida T, Takeuchi K, Watanabe F, Maruyama Y, Andoh A, Tsujikawa T, Fujiyama Y, Mitsuyama K, Sata M, et al. Curcumin maintenance therapy for ulcerative colitis: randomized, multicenter, double-blind, placebo-controlled trial. Clin Gastroenterol Hepatol 2006;4:1502–1506. [PubMed: 17101300]

Heath DD, Pruitt MA, Brenner DE, Rock CL. Curcumin in plasma and urine: quantitation by high-performance liquid chromatography. J Chromatogr B Analyt Technol Biomed Life Sci 2003;783:287–295.

Heath DD, Pruitt MA, Brenner DE, Begum AN, Frautschy SA, Rock CL. Tetrahydrocurcumin in plasma and urine: quantitation by high performance liquid chromatography. J Chromatogr B Analyt Technol Biomed Life Sci 2005;824:206–212.

Hsu HY, Wen MH. Lipopolysaccharide-mediated reactive oxygen species and signal transduction in the regulation of interleukin-1 gene expression. J Biol Chem 2002;277:22131–22139. [PubMed: 11940570]

Ireson C, Orr S, Jones DJ, Verschoyle R, Lim CK, Luo JL, Howells L, Plummer S, Jukes R, Williams M, et al. Characterization of metabolites of the chemopreventive agent curcumin in human and rat hepatocytes and in the rat in vivo, and evaluation of their ability to inhibit phorbol ester-induced prostaglandin E2 production. Cancer Res 2001;61:1058–1064. [PubMed: 11221833]

Ireson CR, Jones DJ, Orr S, Coughtrie MW, Boocock DJ, Williams ML, Farmer PB, Steward WP, Gescher AJ. Metabolism of the cancer chemopreventive agent curcumin in human and rat intestine. Cancer Epidemiol Biomarkers Prev 2002;11:105–111. [PubMed: 11815407]

Kelloff GJ, Crowell JA, Hawk ET, Steele VE, Lubet RA, Boone CW, Covey JM, Doody LA, Omenn GS, Greenwald P, et al. Strategy and planning for chemopreventive drug development: clinical development plan: curcumin. J Cell Biochem Suppl 1996;26:72–85. [PubMed: 9154169]

Kim H, Park BS, Lee KG, Choi CY, Jang SS, Kim YH, Lee SE. Effects of naturally occurring compounds on fibril formation and oxidative stress of beta-amyloid. J Agric Food Chem 2005;53:8537–8541. [PubMed: 16248550]

Kitani K, Yokozawa T, Osawa T. Interventions in aging and age-associated pathologies by means of nutritional approaches. Ann N Y Acad Sci 2004;1019:424–426. [PubMed: 15247057]

Lao CD, Ruffin MT 4th, Normolle D, Heath DD, Murray SI, Bailey JM, Boggs ME, Crowell J, Rock CL, Brenner DE. Dose escalation of a curcuminoid formulation. BMC Complement Altern Med 2006;6:10. [PubMed: 16545122]

Lim GP, Chu T, Yang F, Beech W, Frautschy SA, Cole GM. The curry spice curcumin reduces oxidative damage and amyloid pathology in an Alzheimer transgenic mouse. J Neurosci 2001;21:8370–8377. [PubMed: 11606625]

Lim GP, Yang F, Chu T, Chen P, Beech W, Teter B, Tran T, Ubeda O, Ashe KH, Frautschy SA, et al. Ibuprofen suppresses plaque pathology and inflammation in a mouse model for Alzheimer's disease. J Neurosci 2000;20:5709–5714. [PubMed: 10908610]

Liu A, Lou H, Zhao L, Fan P. Validated LC/MS/MS assay for curcumin and tetrahydrocurcumin in rat plasma and application to pharmacokinetic study of phospholipid complex of curcumin. J Pharm Biomed Anal 2006;40:720–727. [PubMed: 16316738]

Marcu MG, Jung YJ, Lee S, Chung EJ, Lee MJ, Trepel J, Neckers L. Curcumin is an inhibitor of p300 histone acetylatransferase. Med Chem 2006;2:169–174. [PubMed: 16787365]

Montine KS, Quinn JF, Zhang J, Fessel JP, Roberts LJ 2nd, Morrow JD, Montine TJ. Isoprostanes and related products of lipid peroxidation in neurodegenerative diseases. Chem Phys Lipids 2004;128:117–124. [PubMed: 15037157]

Okada K, Wangpoengtrakul C, Tanaka T, Toyokuni S, Uchida K, Osawa T. Curcumin and especially tetrahydrocurcumin ameliorate oxidative stress-induced renal injury in mice. J Nutr 2001;131:2090–2095. [PubMed: 11481399]

Ono K, Hirohata M, Yamada M. Ferulic acid destabilizes preformed beta-amyloid fibrils in vitro. Biochem Biophys Res Commun 2005;336:444–449. [PubMed: 16153607]

Pan MH, Huang TM, Lin JK. Biotransformation of curcumin through reduction and glucuronidation in mice. Drug Metab Dispos 1999;27:486–494. [PubMed: 10101144]

Pan MH, Lin-Shiau SY, Lin JK. Comparative studies on the suppression of nitric oxide synthase by curcumin and its hydrogenated metabolites through down-regulation of IkappaB kinase and NFkappa B in macrophages. Biochem Pharmacol 2000;60:1665–1676. [PubMed: 11077049]

Pendurthi UR, Williams JT, Rao LV. Inhibition of tissue factor gene activation in cultured endothelial cells by curcumin. Suppression of activation of transcription factors Egr-1, AP-1, and NF-kappa B. Arterioscler Thromb Vasc Biol 1997;17:3406–3413. [PubMed: 9437186]

Puig B, Gomez-Isla T, Ribe E, Cuadrado M, Torrejon-Escribano B, Dalfo E, Ferrer I. Expression of stress-activated kinases c-Jun N-terminal kinase (SAPK/JNK-P) and p38 kinase (p38-P), and tau

hyperphosphorylation in neuritis surrounding betaA plaques in APP Tg2576 mice. Neuropathol Appl Neurobiol 2004;30:491–502. [PubMed: 15488025]

Sharma RA, Euden SA, Platton SL, Cooke DN, Shafayat A, Hewitt HR, Marczylo TH, Morgan B, Hemingway D, Plummer SM, et al. Phase I clinical trial of oral curcumin: biomarkers of systemic activity and compliance. Clin Cancer Res 2004;10:6847–6854. [PubMed: 15501961]

Sugiyama Y, Kawakishi S, Osawa T. Involvement of the beta-diketone moiety in the antioxidative mechanism of tetrahydrocurcumin. Biochem Pharmacol 1996;52:519–525. [PubMed: 8759023]

Thiyagarajan M, Sharma SS. Neuroprotective effect of curcumin in middle cerebral artery occlusion induced focal cerebral ischemia in rats. Life Sci 2004;74:969–985. [PubMed: 14672754]

Wang Q, Walsh DM, Rowan MJ, Selkoe DJ, Anwyl R. Block of long-term potentiation by naturally secreted and synthetic amyloid beta-peptide in hippocampal slices is mediated via activation of the kinases c-Jun N-terminal kinase, cyclin-dependent kinase 5, and p38 mitogen-activated protein kinase as well as metabotropic glutamate receptor type 5. J Neurosci 2004;24:3370–3378. [PubMed: 15056716]

Wang YY, Pan MH, Cheng AL, Lin LI, Ho YS, Hsieh CY, Lin JK. Stability of curcumin in buffer solutions and characterization of its degradation products. J Pharm Biomed Anal 1997;15:1867–1876. [PubMed: 9278892]

Weber WM, Hunsaker LA, Gonzales AM, Heynekamp JJ, Orlando RA, Deck LM, Vander Jagt DL. TPA-induced up-regulation of activator protein-1 can be inhibited or enhanced by analogs of the natural product curcumin. Biochem Pharmacol 2006;72:928–940. [PubMed: 16934760]

Wu A, Ying Z, Gomez-Pinilla F. Dietary curcumin counteracts the outcome of traumatic brain injury on oxidative stress, synaptic plasticity, and cognition. Exp Neurol 2006;197:309–317. [PubMed: 16364299]

Yang F, Lim GP, Begum AN, Ubeda OJ, Simmons MR, Ambegaokar SS, Chen PP, Kayed R, Glabe CG, Frautschy SA, et al. Curcumin inhibits formation of amyloid beta oligomers and fibrils, binds plaques, and reduces amyloid in vivo. J Biol Chem 2005;280:5892–5901. [PubMed: 15590663]

## ABBREVIATIONS

AD, Alzheimer's disease
IL, interleukin
pJNK, phospho-JNK, c-Jun $NH_2$-terminal kinase
JNK, c-Jun $NH_2$-terminal kinase
iNOS, inducible nitric-oxide synthase
8-iso-$PGE_{2\alpha}$, 8-iso-prostaglandin $E_2\alpha$
TC, tetrahydrocurcumin
LPS, lipopolysaccharide
Aβ, β-amyloid peptide
gav, gavage
PBS, phosphate-buffered saline
PMSF, phenylmethylsulfonyl fluoride
HFIP, 1,1,1,3,3,3-hexafluoro-2-propanol
LDH, lactate dehydrogenase
DMEM, Dulbecco's modified Eagle's medium
BSA, bovine serum albumin
CNS, central nervous system
Curc, curcumin
HPLC, high-performance liquid chromatography
LC/MS/MS, liquid chromatography-tandem mass spectrometry
MRM, multiple reaction monitoring
ELISA, enzyme-linked immunosorbent assay
TBS, Tris-buffered saline
GFAP, glial fibrillary acidic protein
ANOVA, analysis of variance

TBS-T, Tris-buffered saline/Tween 20
GI, gastrointestinal
NT, nitrotyrosine
APP, amyloid precursor protein
PC, parent compound

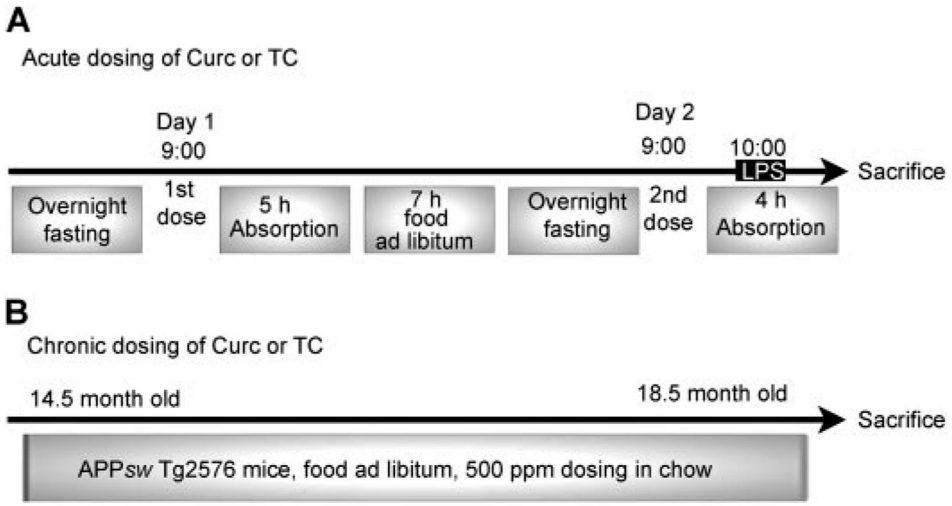


**Fig. 1.**

Schematic paradigms of curcumin and TC treatments. A, mice were treated with Curc or TC by gav, i.p., or i.m. using doses of 0.4, 0.4, or 0.2 μmol (148, 148, or 73.4 μg), respectively. B, aged Tg2576 APP*sw* transgenic mice were fed diets ad libitum with or without curcumin and TC for 4 months at 500 ppm (500 mg/kg chow).

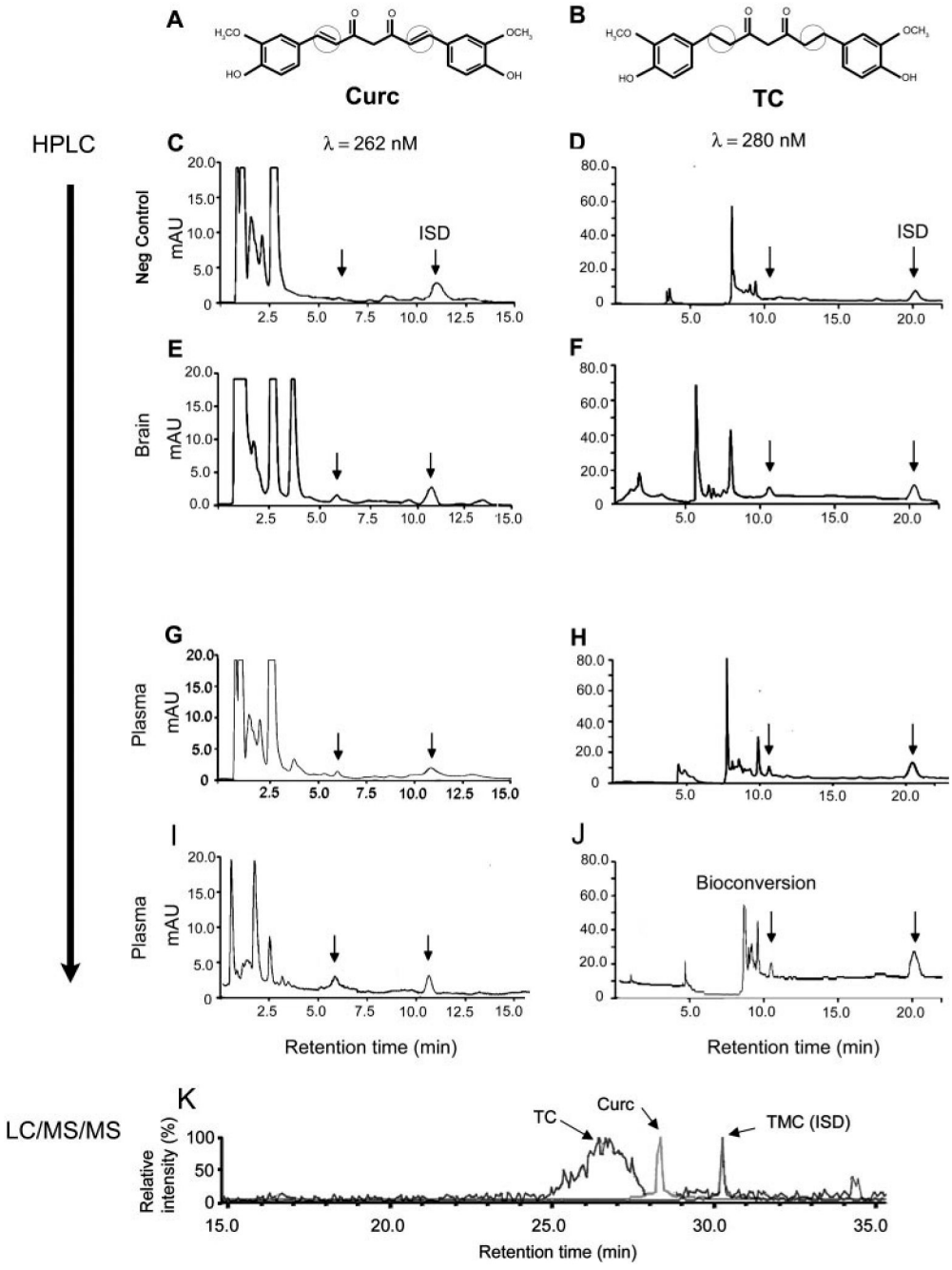


**Fig. 2.**

Detection of curcumin or TC in plasma and brain after acute injection or chronic feeding. Structural differences between curcumin (A) and TC (B) are indicated by circles, highlighting the presence (curcumin) or absence (TC) of diketone bridge. HPLC chromatograms with UV detection for plasma (C–D and G–J) and brain (E and F) are shown for curcumin (left) and TC (right). Control samples only showed the ISD peak, with no TC or curcumin peaks (C and D). At 262 nm, curcumin was detected at peak retention time 5.56 min, and ISD at 10.898 min (E, G, and I), whereas TC was detected at 10.6 min and ISD at 19.9 min (F, H, and J). mAU, milliabsorbance unit. I and J, chromatograms of plasma collected from mice fed for 4-month ad libitum feeding with curcumin in chow (2000 ppm; $n = 5$) revealed predominantly curcumin

(I), but also significant bioconversion to TC (J). LC/MS/MS-MRM chromatograms of a brain extract from mice chronically fed the parent compound curcumin (K) show clear peaks for Curc (*m/z* 371→149 transition) and TMC (*m/z* 395.2→365.1 transition), and in addition a peak for TC (*m/z* 371.1→235 transition), which elutes as an earlier and broader peak on the chromatographic system used. ISD, internal standard.

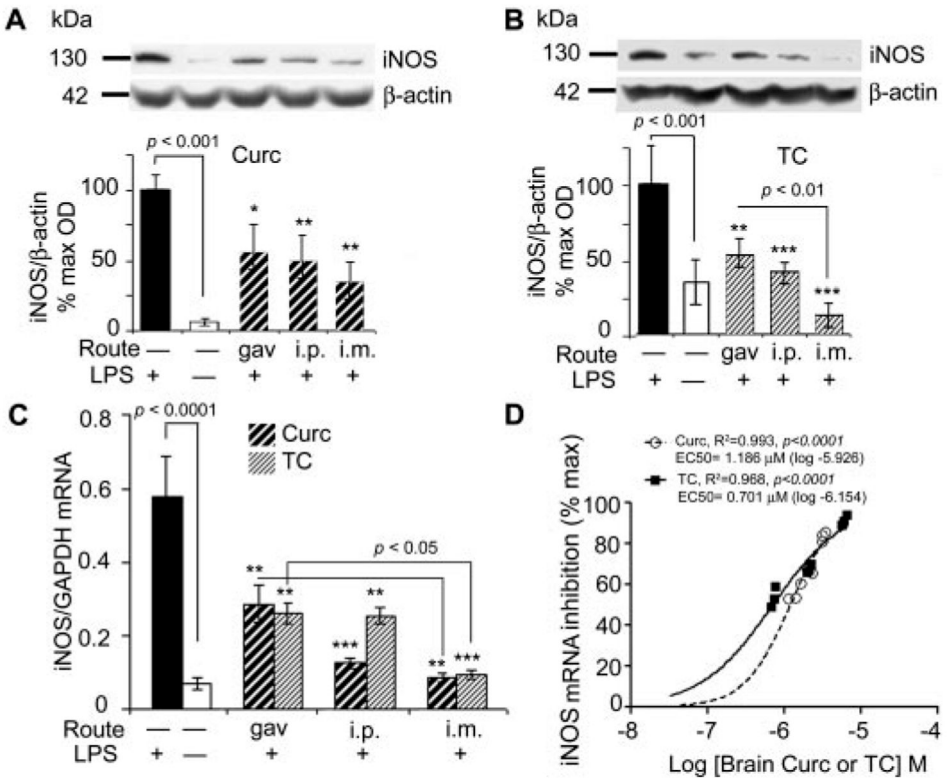


**Fig. 3.**

Curcumin and TC suppressed LPS-induced iNOS protein and mRNA. Mice injected with LPS or vehicle, were sacrificed 4 h after administration of curcumin (A) or TC (B), and the supernatant of TBS-extracted brains was electrophoresed on Western blot and immunostained with anti-iNOS and β-actin. Representative lanes and their densitometric quantitation are shown. C, RNA was extracted from brain and measured for iNOS mRNA using quantitative RT-PCR. D, percentage of iNOS inhibition was regressed on curcumin or TC concentrations. Closed circles, curcumin; open circles, TC. Values shown are the amount of iNOS mRNA as the mean ± S.D. *, $p < 0.05$; **, $p < 0.01$; and ***, $p < 0.001$ represent a significant difference compared with positive controls (LPS treatment alone; $n = 4$).

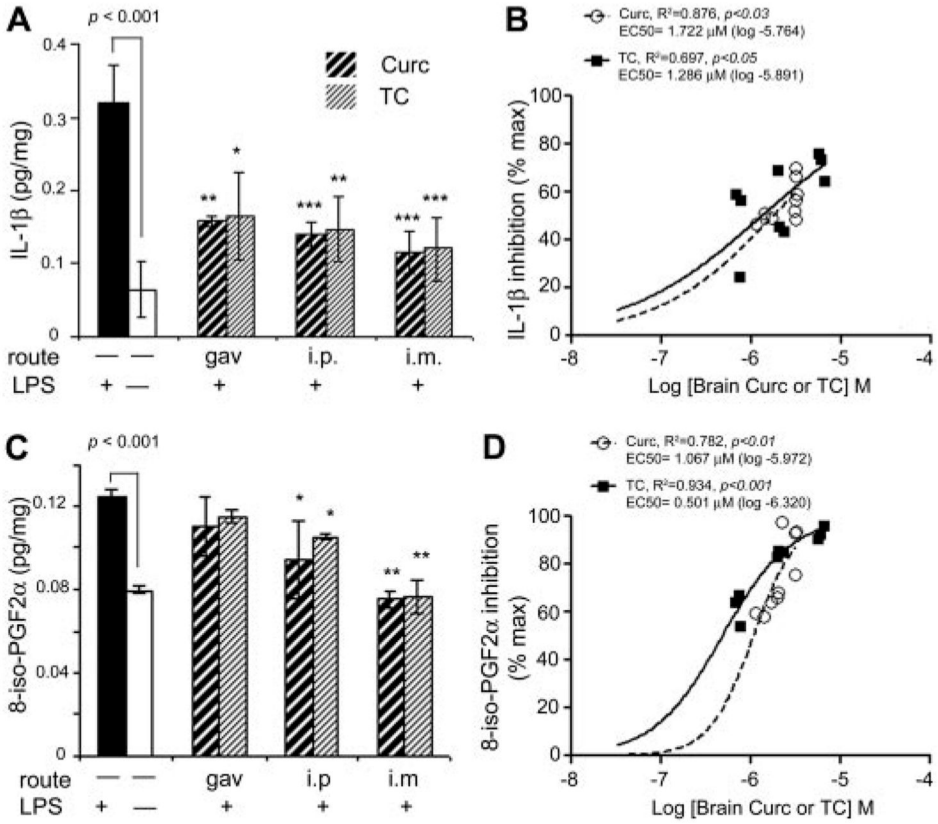


**Fig. 4.**

Acute injection of TC or curcumin similarly attenuated LPS induced-IL-1β or F2 isoprostane. A, quantitation of IL-1β levels in mouse brain homogenates was determined by sandwich ELISA. LPS injection (i.p.) increased IL-β levels more than 6-fold, an effect that was partially (>50%) suppressed by acute administration of either curcumin or TC, regardless of route of administration. B, either curcumin or TC levels correlated positively with percentage of IL-1β inhibition. C, lipid extracts of brain were measured for 8-iso-$PGF_2\alpha$ by ELISA. The 40% increase in 8-iso-$PGF_2\alpha$ caused by LPS was partially reduced by i.p. injection and completely suppressed by i.m injection of either compound. D, brain curcumin or TC correlated positively with brain F2 isoprostane inhibition. Values shown are the mean ± S.D. *, $p < 0.05$; **, $p < 0.01$; and ***, $p < 0.001$ represent significant difference compared with positive controls (LPS treatment alone; $n = 4$).

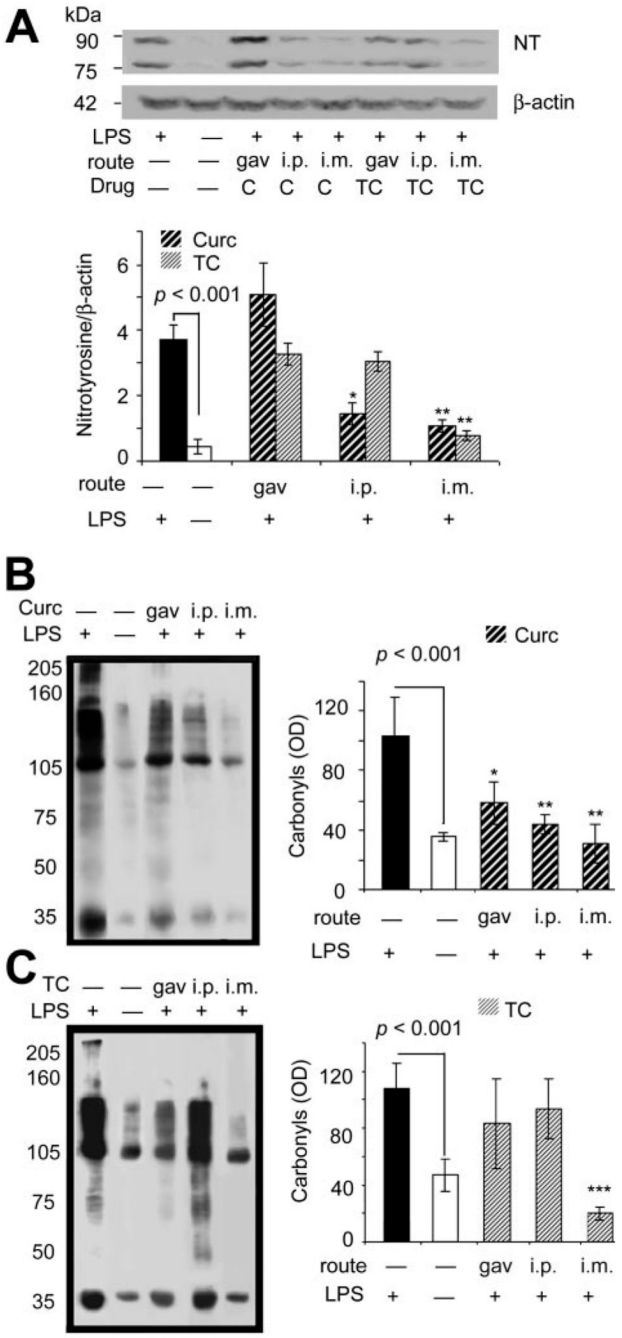


**Fig. 5.**

Acute curcumin or TC similarly suppresses LPS induction of brain NT, but curcumin is more effective at suppressing carbonyls. A, NT proteins increased more than 7-fold after LPS from mouse brain homogenates measured by Western blot with anti-nitrotyrosine antibody and normalized to β-actin. Injection (i.m.) of either compound suppressed NT induction. Injection (i.p.) of curcumin partially suppressed NT induction, whereas i.p. injection of TC did not affect NT induction. Oxidized protein levels of brain were determined in the lysis-extracted supernatant of the TBS-insoluble pellet using Oxyblot analysis with an anti-DNP antibody. Representative lanes are shown and quantified for curcumin- (B) or TC-(C) fed mice. Values

shown are the mean ± S.D. *, $p < 0.05$ and **, $p < 0.01$ represent a significant difference compared with positive controls (LPS treated alone; $n = 4$).

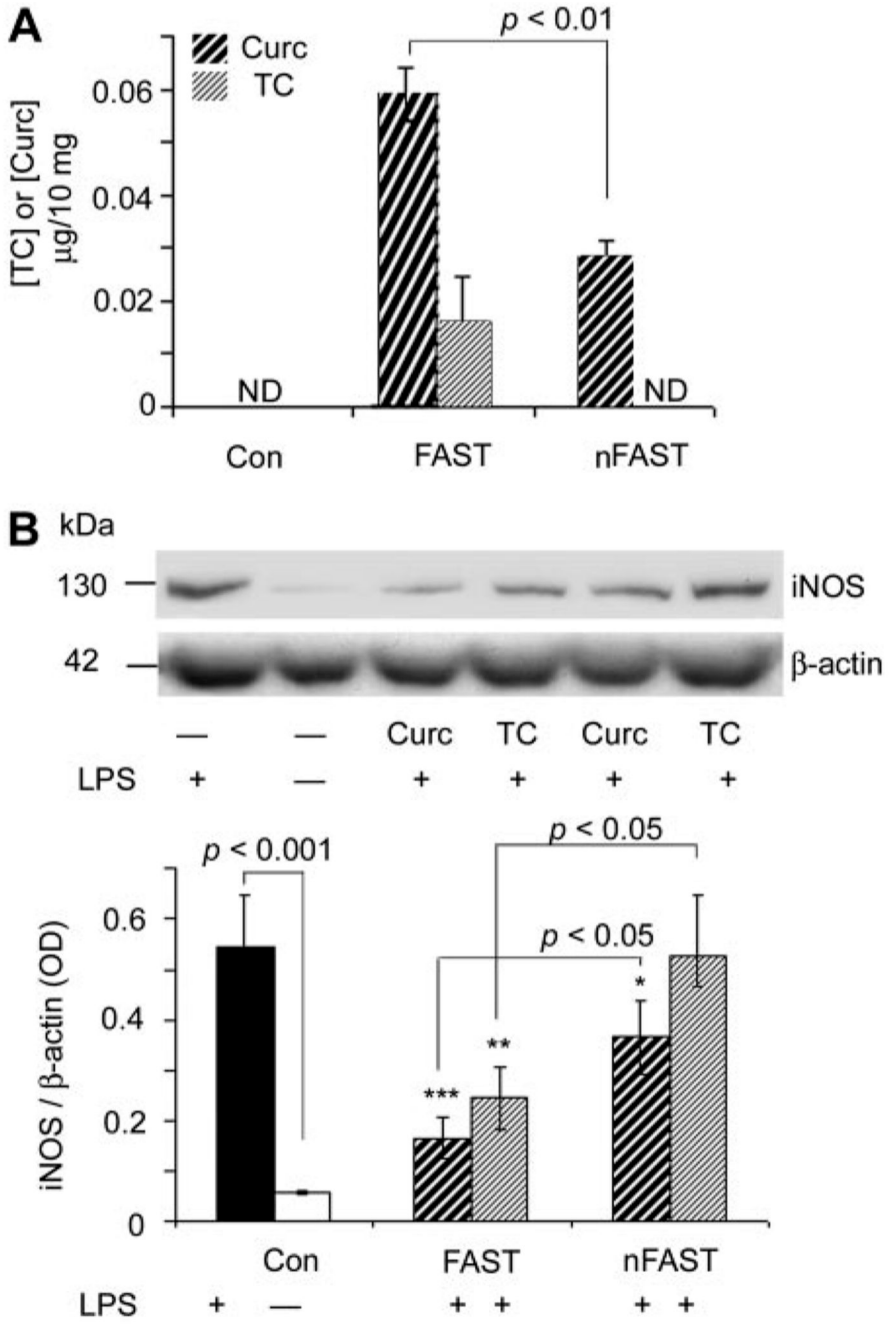


**Fig. 6.**

Brain levels and efficacy of curcumin and TC administered by gavage are increased by fasting. Four hundred and eighty micrograms of curcumin or TC was administered to mice by gavage with fasting (FAST) or nonfasting (nFAST). After 4 h, brains were removed, and then they were prepared for the analysis of curcumin and TC levels by HPLC (A) and iNOS protein (B) measured by Western blot of iNOS and normalized with β-actin (endogenous control). When administered with food, brain curcumin levels were not detectable, and TC levels were reduced 50% compared with if mice had fasted. Curcumin and TC reduced iNOS less if administered with food. Values shown are the mean ± S.D. *, $p < 0.05$ and **, $p < 0.01$ represent a significant

difference compared with control (con, untreated; $n = 4$), curcumin, or TC by gav ($n = 4$, each treatment). ND, not detectable.

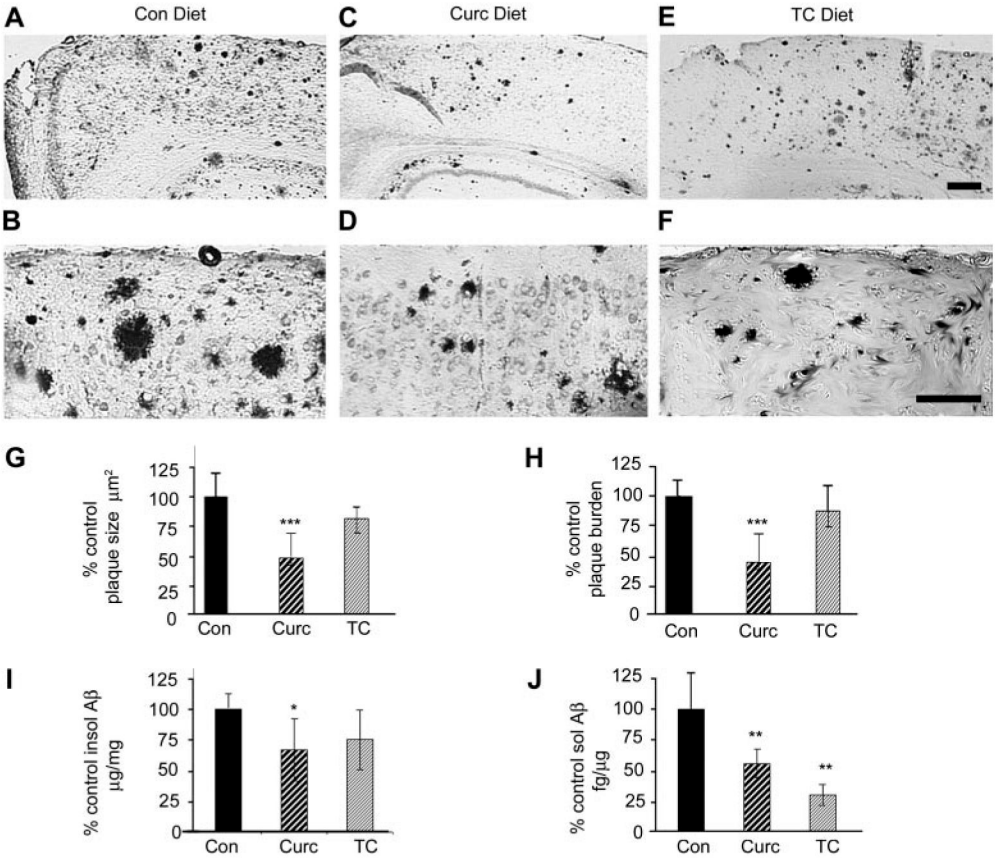


**Fig. 7.**

Dietary curcumin seems more effective than TC in reducing plaque pathology in the Tg2576 APP*sw* mouse, but both reduce soluble Aβ levels. Curcumin or TC was administered to aged Tg2576 mice for 4 months (12–16 months old) in the chow (500 ppm) during accelerated plaque deposition. Representative micrographs stained with antibodies to Aβ (DAE; anti-Aβ1-13). Compared with Tg+ mice on control diet (A and B), mice on curcumin diet showed a noticeable reduction in plaque size and number (C and D). However, sections from mice on dietary TC (E and F) showed plaque distribution similar to those from mice on control diet. Although image analysis quantification confirmed that dietary curcumin could reduce plaque size (G) and plaque burden (H), dietary TC seemed to have no impact on plaque pathology. I, insoluble (guanidine-insoluble) and soluble Aβ (TBS-soluble) in cortical homogenates were also evaluated by Aβ sandwich ELISA. Curcumin, but not TC, reduced Aβ levels in detergent-insoluble fraction. J, in contrast, both drugs suppressed soluble Aβ levels (in TBS-extracted brain homogenates), with a trend for TC being more potent. Magnification bar, 75 µm. Statistical analysis of Western data were performed by one-way ANOVA and immunohistochemistry data by 2 × 2 ANOVA (treatment × brain region), and values shown are the mean ± S.D. *, $p < 0.05$; **, $p < 0.01$; and ***, $p < 0.001$ represent significant difference of control ($n = 5$) and standard diet ($n = 5$) compared with curcumin ($n = 9$) and TC ($n = 7$) treatment of Tg+ mice, respectively.

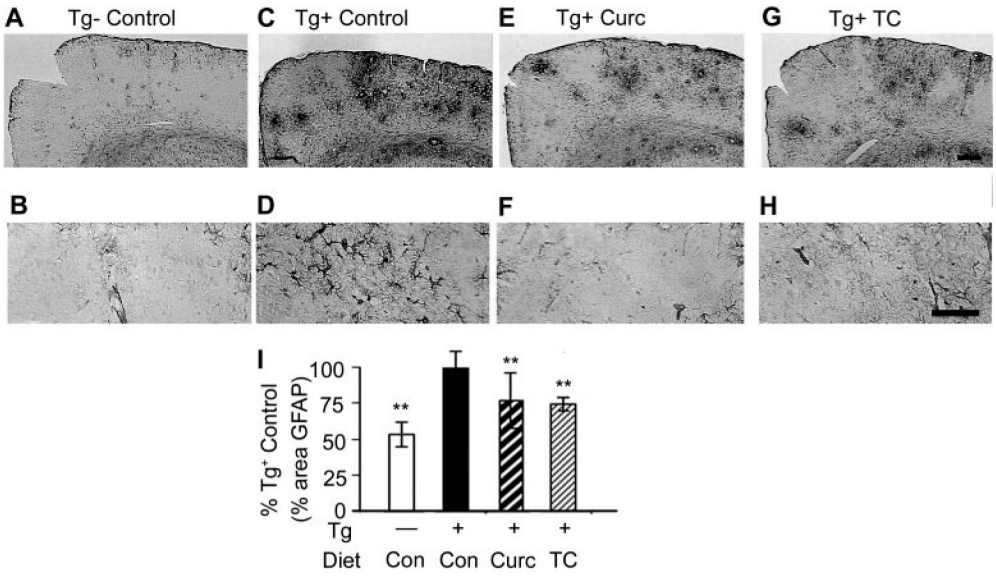


**Fig. 8.**

Curcumin or TC diets ameliorated Tg2576-dependent glial activation. Micrographs demonstrated that compared with brains of Tg− mice (A and B), brains of Tg+ mice (C and D) showed increased staining for GFAP. Compared with Tg+ mice fed control diet, Tg+ mice fed either curcumin (E and F) or TC (G and H) in chow showed reduced GFAP (glial activation). Quantification of percentage GFAP staining demonstrated significant attenuation of transgene-dependent gliosis by both TC and curcumin (I). Values shown are the mean ± S.D.**, $p < 0.01$ represents significant difference of curcumin ($n = 9$) or TC ($n = 7$) treatment of mice compared with control diet ($n = 5$). Magnification bar, 75 μm.

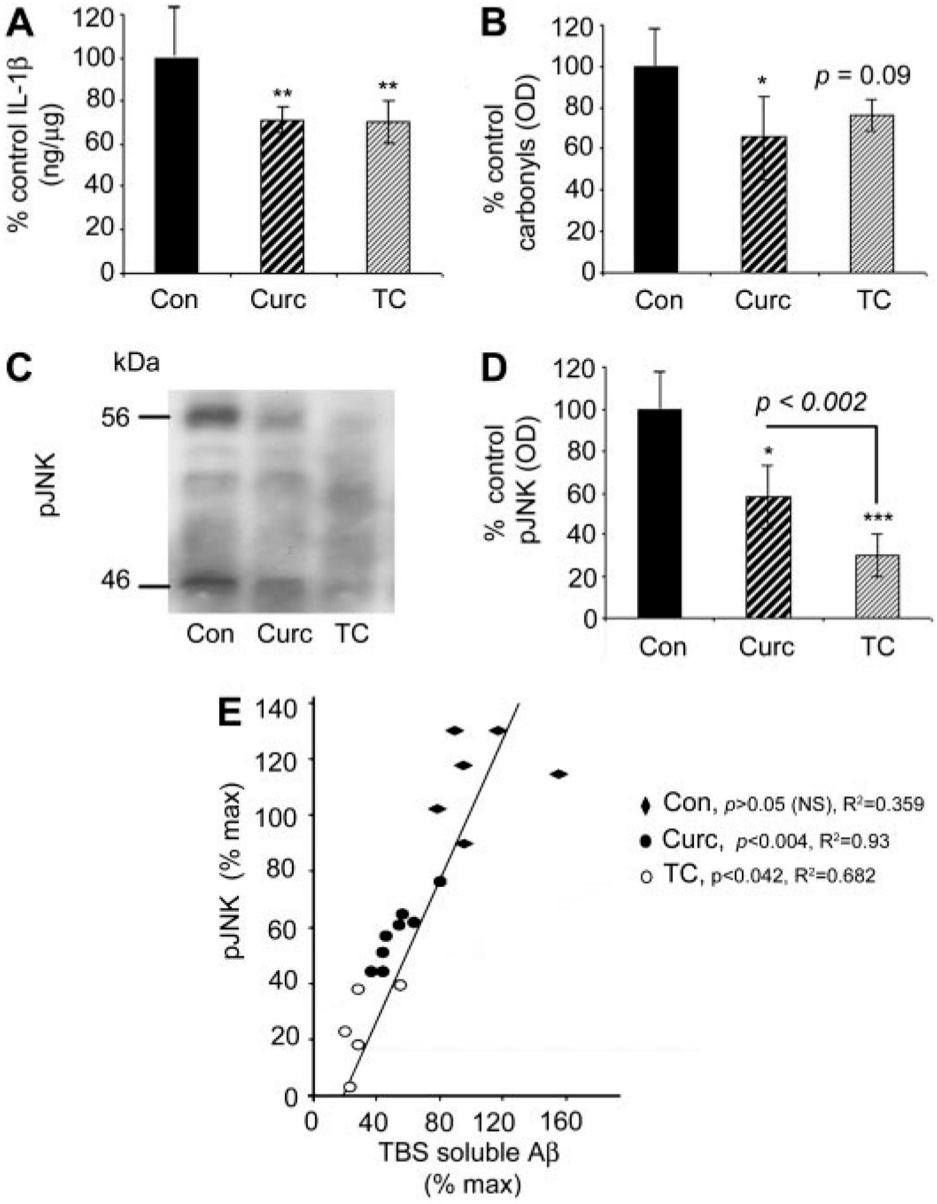


**Fig. 9.**

In APP*sw* Tg2576 mice, both dietary curcumin or TC similarly reduced IL-1β and pJNK, whereas curcumin, but not TC, reduced carbonyls. A, compared with Tg+ mice on control diet, mice fed curcumin or TC showed 25% reduction in IL-1β levels as measured by sandwich ELISA of TBS-extracted supernatant fraction of brain homogenate. B, compared with Tg+ mice on control diet brain curcumin reduced carbonyls measured on Western with anti-DNP antibody from the detergent buffer-extracts of brain homogenates. Although TC-fed mice showed a trend for reduction, it was not statistically significant. C, Western analysis of main pJNK bands of 46 and 56 kDa showed that compared with mice fed control diet, mice fed TC or curcumin showed reduced pJNK. D, densitometric quantification showed that compared with control fed Tg+ mice, mice fed curcumin or TC showed reductions in pJNK, with TC showing the greater reduction. E, pJNK was positively correlated with soluble Aβ. Values shown are the mean ± S.D. *, $p < 0.05$; **, $p < 0.01$; and ***, $p < 0.001$ represent significant difference of curcumin ($n = 9$) or TC ($n = 7$) treatment of Tg+ mice with control diet ($n = 5$).

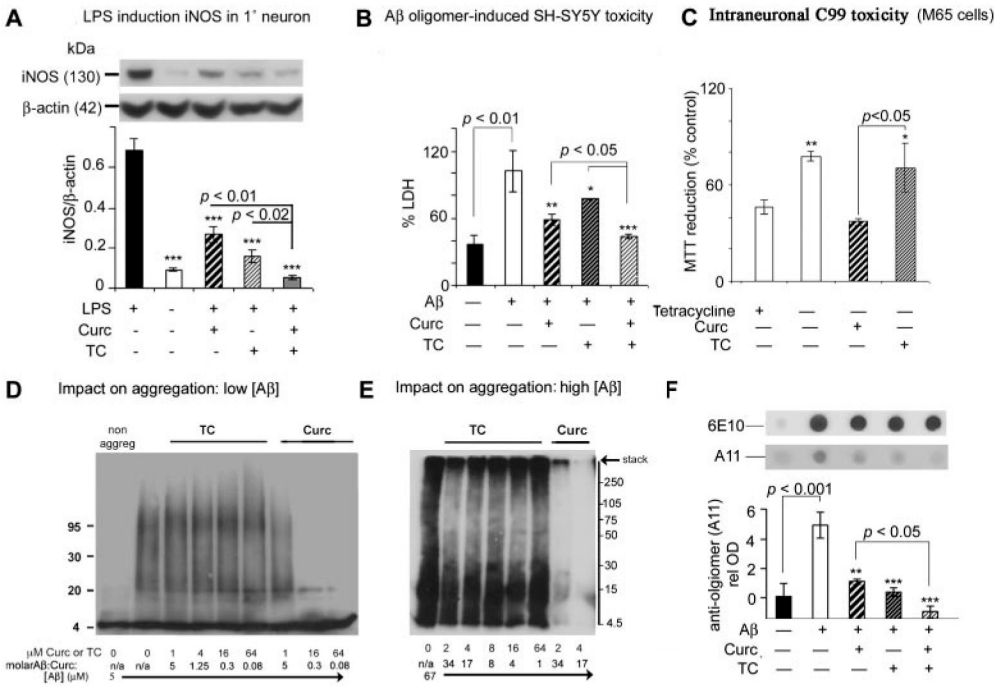


**Fig. 10.**

Differential impact of TC versus curcumin on iNOS, Aβ toxicity and Aβ aggregation in vitro. Primary cortical neuron cultures (A) or the microglial cell line BV-2 (data not shown) were treated with 1 μg/ml LPS, and iNOS protein levels in the detergent-soluble fraction were measured by Western blot with or without curcumin (2.5 μM), TC (2.5 μM), and curcumin + TC (1.25 μM each), using β-actin as an endogenous control to ensure equal protein loading. LPS induction of iNOS was attenuated by curcumin (50%), TC (80%), or combined curcumin + TC (95%). B, attenuation of Aβ42 oligomer (500 nM)-induced toxicity (% maximal LDH) in SH-SY5Y neuroblastoma by pretreatment with curcumin (40%), TC (20%), or curcumin + TC (70%). C, TC, but not curcumin minimized the reduction in viability [3-(4,5-dimethylthiazol-2-yl)-2,5-diphenyltetrazolium reduction] in MC65 neuroblastoma cells caused by intraneuronal expression of C99, 3 days after tetracycline withdrawal. D and E, Western blot for Aβ immunoreactivity bands (6E10) to assess drug effect on aggregation of specific molecular weight oligomers. Impact of cotreatment of TC and curcumin on aggregation of low-dose (5 μM) Aβ (D) or high-dose (67 μM) Aβ (E), initially monomerized with HFIP. F, both TC and curcumin reduced levels of oligomeric-specific antibody A11 during oligomerization of 11 μM Aβ, using starting curcuminoid/Aβ molar ratio of 1.45 to 1. Equal loading is demonstrated by a second dot blot with 6E10. Values shown are the mean ± S.D. *, $p < 0.05$; **, $p < 0.01$; and ***, $p < 0.001$ represent significant differences compared with positive control ($n = 4$) and treatments ($n = 4$).

**TABLE 1**

**Detection of curcumin and TC in plasma and brain after multiple dosing routes**

These data showed brain and plasma levels of curcumin or TC 4 h after administration (by gavage, i.p., and i.m.). The lower limits of detection for curcumin were 35 ng/ml in plasma and 100 ng/g wet tissue in brain, and for TC they were 8 ng/ml in plasma and 250 ng/g wet tissue in brain. Data are presented as mean ± S.D.

| Parent Compound (PC) | Route | Plasma | Plasma | Brain | Brain | Brain-to-Plasma Ratio (PC) |
|---|---|---|---|---|---|---|
| | | μ*g/ml* | μ*M* | μ*g/g tissue* | μ*M* | |
| Vehicle | i.m. | N.D. | N.D. | N.D. | N.D. | N.D. |
| Curc | gav | N.D. | N.D. | 0.519 ± 0.098a | 1.412 | N.D. |
| Curc | i.p. | 0.127 ± 0.035a[a] | 0.345 | 0.739 ± 0.019b | 2.010 | 5.85 |
| Curc | i.m. | 0.238 ± 0.048b | 0.647 | 1.162 ± 0.004c | 3.157 | 4.88 |
| Vehicle | i.m. | N.D. | N.D. | N.D. | N.D. | N.D. |
| TC | gav | N.D. | N.D. | 0.274 ± 0.015d | 0.736 | N.D. |
| TC | i.p. | 0.847 ± 0.019c | 2.302 | 0.765 ± 0.023b | 2.056 | 0.90 |
| TC | i.m. | 0.971 ± 0.092c | 2.639 | 2.234 ± 0.163e | 6.007 | 2.28 |

N.D., not detectable.

[a]Different letters represent statistical differences of means from each other between treatments within route of administration or between routes within treatments; $P < 0.05$.

**TABLE 2**

**Parent and metabolite compounds in plasma and brain after chronic dietary administration**

Curcumin or TC in chow was fed to mice for 4-month duration at 500 ppm (~2.5 mg/day) or 2000 ppm (~10 mg/day). After sacrifice, plasma was collected, animals were perfused, and brains were removed. Plasma values were detected using HPLC, and the lower limits of detection for curcumin and TC were 35 and 8 ng/ml, respectively. Brain levels were measured using LC/MS/MS, and the lower limits of detection were 100 pg/g t for curcumin and 1 ng/g t for TC. Data represent mean ± S.D.

| Dose Chow | PC | Plasma Curc | Plasma TC | Brain Curc | Brain TC | Brain-to-Plasma Ratio (PC) |
|---|---|---|---|---|---|---|
| | | *μg/ml or (μM)* | | *μg/g t or (μM)* | | |
| 0 ppm | Con | N.D. | N.D. | N.D. | N.D. | N.A. |
| 500 ppm | Curc | 0.035 ± 0.014 (0.095 μM) | 0.008 ± 0.001 (0.023 μM) | 0.469 ± 0.220 (1.276 μM) | 0.097 ± 0.008 (0.264 μM) | 13.4 |
| 2000 ppm | Curc | 0.171 ± 0.019 (0.465 μM) | 0.042 ± 0.002 (0.115 μM) | 0.525 ± 0.125 (1.428 μM) | 0.052 ± 0.054 (0.143 μM) | 3.07 |
| 500 ppm | TC | N.D. | 0.270 ± 0.003 (0.734 μM) | N.D. | 0.128 ± 0.019 (0.344 μM) | 0.47 |

N.A., not applicable; N.D., not detectable; t; wet tissue.